Chinese Chemical Letters 33 (2022) 5147–5151

Contents lists available at ScienceDirect

Chinese Chemical Letters

journal homepage: www.elsevier.com/locate/cclet

Ligand-field regulated superalkali behavior of the aluminum-based clusters with distinct shell occupancy

Jun Li[a,1], Mingwei Cui[a,1], Huan Yang[b], Jing Chen[a], Shibo Cheng[a,*]

[a] School of Chemistry and Chemical Engineering, Shandong University, Ji'nan 250100, China
[b] School of Physics, Shandong University, Ji'nan 250100, China

ARTICLE INFO

Article history:
Received 7 January 2022
Revised 10 February 2022
Accepted 15 February 2022
Available online 19 February 2022

Keywords:
Superalkali
Density functional theory
Ligand-field strategy
Aluminum-based cluster
Electronic property

ABSTRACT

Protecting clusters from coalescing by ligands has been universally adopted in the chemical synthesis of atomically precise clusters. Apart from the stabilization role, the effect of ligands on the electronic properties of cluster cores in constructing superatoms, however, has not been well understood. In this letter, a comprehensive theoretical study about the effect of an organic ligand, methylated *N*-heterocyclic carbene ($C_5N_2H_8$), on the geometrical and electronic properties of the aluminum-based clusters XAl_{12} (X = Al, C and P) featuring different valence electron shells was conducted by utilizing the density functional theory (DFT) calculations. It was observed that the ligand can dramatically alter the electronic properties of these aluminum-based clusters while maintaining their structural stability. More intriguingly, different from classical superatom design strategies, the proposed ligation strategy was evidenced to possess the capability of remarkably reducing the ionization potentials (IP) of these clusters forming the ligated superalkalis, which is regardless of their shell occupancy. The charge transfer complex formed during the ligation process, which regulates the electronic spectrum through the electrostatic Coulomb potential, was suggested to be responsible for such an IP drop. The ligation strategy highlighted here may provide promising opportunities in realizing the superatom synthesis in the liquid phase.

Due to the quantum confinement, atomic clusters, containing several to thousands of atoms, usually present unique properties, which represents a new phase of materials bridging the gap between the atoms and bulk materials. It is acknowledged that the composition and structure both have significant impacts on the cluster's properties [1,2]. Particularly, a class of atomic clusters has been discovered to have the characteristics in mimicking the chemistry of the atom in the periodic table, termed as "superatoms" [3–5]. Since they share similar properties with atoms and expand the definition of an element to involve species that behave as entities, the superatoms could be utilized to build a three-dimensional (3D) periodic table [6]. Serving as building blocks, these superatoms are also potential candidates in forming novel cluster-assembled materials, which can be used in the energy storage and conversion [7–12].

In the development of the superatoms, different categories have been proposed, such as superalkali [10,13], superhalogen [12,14,15], rare-earth superatoms [16] and magnetic superatoms [17,18]. Among them, the superalkali with the adiabatic ionization potentials (AIPs) lower than those of alkali atoms (3.89-5.39 eV) and superhalogen, whose adiabatic electron affinities (AEAs) are higher than those of halogen elements (3.06-3.62 eV), are two most important series that could mimic the properties of alkali and halogen atoms, respectively. Over the past several decades, various electron counting rules, such as the Jellium model [19], the octet rule [20,21], the Wade-Mingos rule [22,23], the 18-electron rule [24], the aromatic rule [25,26] and others, have been successfully applied in constructing superatomic clusters. Yet, challenges remain in designing and synthesizing these special clusters since these classical models highly correlate with the intrinsic properties of clusters, *e.g.*, the elemental composition and the shell filling, which are relatively difficult to modulate in the chemical synthesis. In other words, conventional design strategies mainly depend on how the superatomic states of the superatoms are filled. Under such circumstance, an interesting question is whether one can control the electronic properties of clusters by only regulating their external environment rather than altering their intrinsic characteristics? That is to say, is it possible to go beyond the traditional shell effect to manipulate the clusters' electronic properties, for example, to turn the superhalogen into a superalkali, or transform the clusters featuring closed shell which obeys the Jellium

* Corresponding author.
E-mail address: shibocheng@sdu.edu.cn (S. Cheng).
[1] These authors contributed equally to this work.

https://doi.org/10.1016/j.cclet.2022.02.039
1001-8417/

model into a superalkali one? This represents a substantial step towards the chemical synthesis of atomically precise superatoms. Fortunately, it is well-established that coating clusters with ligands is a practical way that has been proved by numerous experiments [27–31], where ligands were used to stabilize the cluster cores. Our previous works have also proved that it is effective to tailor the electronic properties of metal clusters by applying suitable ligands [10,32,33].

In the present letter, we combined the ligation strategy, which is wildly used in the liquid-phase cluster synthesis, with the bare Al_{13} and doped XAl_{12} (X = C and P) clusters to examine the ligand-field effect on the electronic properties of these clusters. Considering the limitations of traditional electron counting rules, which are inseparable from the shell effect of the cluster itself or its unique geometric configuration, what we interest most here is whether it is attainable to transcend the shell effect and produce superalkalis without changing the cluster's electronic configuration and stability. Our long-term experience in designing superatoms [10,12,16,32-35] and the achievements of our peers [36–38] inspire us that it may achieve the intended purpose by connecting the electron-donating ligand to the cluster core. Thus, one class of typical ligands, *N*-heterocyclic carbenes (NHCs) that have been successfully applied in the organic chemistry and coordination chemistry, was adopted here. Not only can NHCs serve as the reagents and catalysts in organic chemistry, such as the transesterification, nucleophilic aromatic substitution, and cycloaddition reaction, but they also play an important role in the coordination chemistry and organometallic reaction [39–41]. To simplify the calculations, we chose the less "bulky" one, 1,3-dimethylimidazol-2-ylidene ($C_5N_2H_8$), a neutral compound containing a divalent carbon atom with an incomplete electron octet. Successive attachment of $C_5N_2H_8$ on these aluminum-based clusters featuring different valence electrons, *i.e.*, 39, 40 and 41e, was attempted to examine its effect on the clusters' geometrical and electronic properties. Furthermore, the mechanism for the change in the electronic property and the interaction between the ligand orbital and superatomic states of these clusters were also discussed.

All calculations were performed by using the Gaussian 09 program package [42]. The PBE0 [43] functional coupled with the def2-SVP basis set [44] was employed to obtain the optimized structures of $XAl_{12}(C_5N_2H_8)_n$ (X = Al, C and P; n = 1-3). Various positions of ligands and spin structures were checked and compared to ensure the ground states of these clusters, and no imaginary frequencies were observed. To evaluate the AIP and AEA values, geometries of all the neutral, cationic, and anionic clusters were optimized. Our calculated EA of Al_{13} is 3.54 eV. This result is in excellent agreement with the experimental measurement (3.57 ± 0.05 eV) [45], validating the accuracy of the present level of theory. The Hirshfeld, Mulliken and NBO charge were analyzed to estimate the amount of charge transfer between the ligand and the metallic core in the ligated aluminum-based clusters [46,47]. The electrostatic potential (ESP) analysis, molecular orbital (MO) analysis, and charge decomposition analysis (CDA) were also conducted and visualized via the Multiwfn [48] and VMD [49] softwares.

Considering numerous possible configurations and spin multiplicities, we first optimized the ground states of $XAl_{12}(C_5N_2H_8)_n$ (X = Al, C and P; n = 1-3) clusters at the PBE0/def2-SVP level. Their neutral and charged ground-state structures are depicted in Fig. 1 and Figs. S1 and S2 (Supporting information), respectively. Here, the XAl_{12} clusters featuring 39, 40 and 41 valence electrons, respectively, were adopted as the cluster cores since we want to explore whether the effect of $C_5N_2H_8$ in regulating the clusters' electronic properties is independent of their shell fillings. The 40-electron clusters, *i.e.*, CAl_{12} and Al_{13}^-, share the identical I_h symmetry, whose shell configurations are $(1S)^2(1P)^6(1D)^{10}(2S)^2(1F)^{14}(2P)^6$ based on the Jellium

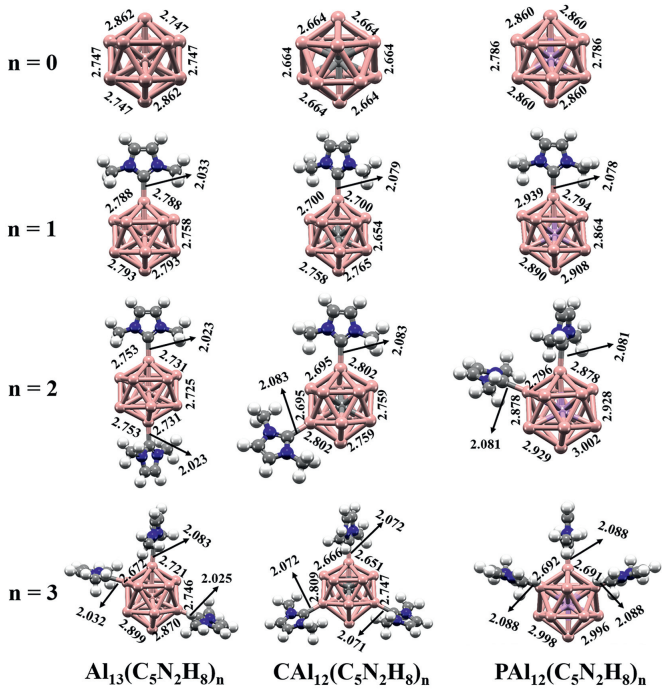

Fig. 1. Optimized ground states of $XAl_{12}(C_5N_2H_8)_n$ (X = Al, C and P; n = 1-3) calculated at the PBE0/def2-SVP level of theory. The Al-Al and Al-C bond lengths are shown in Å.

model. And, once the center atom of CAl_{12} is replaced by Al or P, the electronic shell rearranges to $...(1D)^{10}(2S)^2(2P)^6(1F)^{13}$ or $...(1D)^{10}(2S)^2(1F)^{14}(2P)^6(1G)^1$, respectively. As shown in Fig. 1, there is a significant change in the bond lengths of the doped clusters, representing a symmetry lowering in these clusters compared with the original CAl_{12} cluster. Specifically, compared with CAl_{12}, the average bond lengths from the central atom to the surface Al atoms of Al_{13} and PAl_{12} increase from 2.53 Å to 2.67 and 2.65 Å. Such a change in geometries can be attributed to the Jahn-Teller distortion.

The structures and relative stability of the ligated complexes were also investigated. As shown in Fig. 1, the structures are quite different when the 2nd $C_5N_2H_8$ ligand was connected to XAl_{12} (X = Al, C and P). In $Al_{13}(C_5N_2H_8)_2$, the 2nd ligand occupies the para-position, while the two ligands are in the ortho- and meta-positions of $PAl_{12}(C_5N_2H_8)_2$ and $CAl_{12}(C_5N_2H_8)_2$, respectively. Furthermore, when these clusters bind with the 3rd ligand, $Al_{13}(C_5N_2H_8)_3$ stabilizes in an ortho-position structure, while the other two tendencies remain unchanged. With the continuous attachment of the ligand, the symmetry of the cluster gradually decreases. Surprisingly, although the symmetrical distortion takes place during the ligation, the average bond lengths between the central atoms X and the surficial Al atoms in different ligated clusters scarcely change (Fig. 2a). Thus, it seems that the geometry of XAl_{12} remains almost unchanged after interacting with $C_5N_2H_8$. Does this imply that the bonding characteristics and electronic arrangements of the cluster cores have not changed significantly during the ligation process?

To gain the charge transfer behavior between the inner-core and ligands, the Hirshfeld, Mulliken and NBO charge analysis were performed. As summarized in Table S1 (Supporting information), consistent trends and conclusions were reached. Taking the Hirshfeld charge analysis as an example, $\Delta Q_{n-(n-1)}$ represents the charge accumulation on the inner-core with respect to its precursor ligation. It can be seen from Fig. 2b that the charges of all inner cores increase monotonously with the continuous addition of

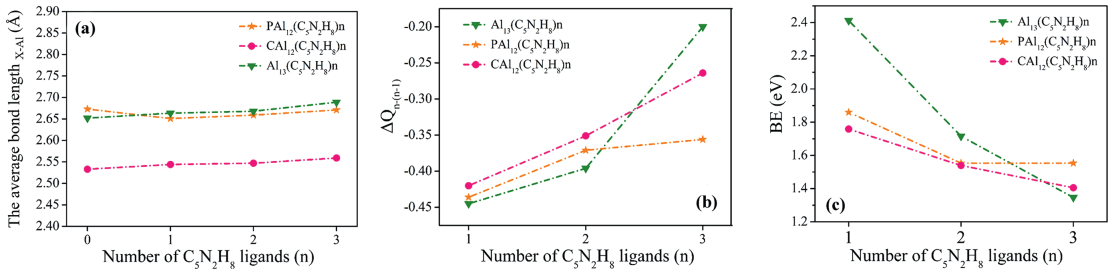

Fig. 2. Calculated (a) average bond lengths between the central atom X to surface Al atoms, (b) accumulated charges of the inner-core clusters, and (c) BEs in $XAl_{12}(C_5N_2H_8)_n$ (X = Al, C and P; n = 1-3).

$C_5N_2H_8$. To understand the overall charge transfer behavior, the total charge transfer amount ΔQ_n, which represents the charge accumulation on the inner core with respect to its bare cluster, was also examined. Based on the present calculations, the total charge transfers to the Al_{13}, CAl_{12} and PAl_{12} cluster cores are 1.05, 1.17 and 1.03e upon the attachment of three $C_5N_2H_8$ ligands, respectively, which clearly demonstrates the electron-donating characteristic of $C_5N_2H_8$. To visualize such charge distribution, the ESP of $XAl_{12}(C_5N_2H_8)_n$ (X = Al, C and P; n = 1-3) were drawn. As shown in Fig. S3 (Supporting information), the surface of the naked cluster is in dark blue, signifying the negative charge accumulation, and the color continues to deepen as the number of $C_5N_2H_8$ increases, which is the same as the results of the charge analysis (Fig. 2b).

To further explore the interactions between $C_5N_2H_8$ and three aluminum-based clusters, the binding energies (BEs) (Fig. 2c) were calculated as:

$$BE = E(XAl_{12}L_{n-1}) + E(L) - E(XAl_{12}L_n) \quad (1)$$

where L = $C_5N_2H_8$, and E presents the total energies of different species. Due to the electron deficiency of Al_{13}, the BE of the 1st ligand attachment to Al_{13} is much larger than those of other two clusters. The calculated BEs are in the range of 1.35-2.41 eV, which are higher than the previous reported PH_3 and CO ligands (0.29-1.17 eV) [10]. This indicates that the interactions between $C_5N_2H_8$ and XAl_{12} (X = Al, C and P) are stronger than those of the CO and PH_3 ligands, which may increase the probability of being obtained in the liquid-phase cluster synthesis. In addition, the energy gap between the highest occupied molecular orbital (HOMO) and the lowest unoccupied molecular orbital (LUMO), marked as H-L gap, is a useful criterion to assess the relative stability of clusters. Generally, clusters with larger H-L gap are more stable and chemically inert [50–52]. The calculated H-L gaps of $XAl_{12}(C_5N_2H_8)_n$ (X = Al, C and P; n = 1-3) are in the range of 1.44-2.84 eV (Table S2 in Supporting information). These high H-L gaps are comparable with that of C_{60} (1.70 eV) [53], demonstrating the high stability of these ligated clusters.

We now turn our attention in clarifying whether such strong ligation process can alert the electronic properties of these clusters since all calculated BEs are relatively large (Fig. 2c). Here, two important electronic properties, *i.e.*, AIP and AEA, of ligated clusters were estimated, which are defined as:

$$AIP = E(\text{ground state of cation}) - E(\text{ground state of neutral}) \quad (2)$$

$$AEA = E(\text{ground state of neutral}) - E(\text{ground state of anion}) \quad (3)$$

The theoretical AEA and AIP values are listed in Table S3 (Supporting information). As mentioned above, Al_{13} (39e) lacks an electron to satisfy the closed shell. Therefore, Al_{13} is expected to exhibit superatomic character analogous to halogen atoms. Our calculated AEA value of Al_{13} is 3.54 eV, which is similar to that of the halogen. On the contrary, PAl_{12} (41e) is easy to lose an electron, showing the property of the superalkali metal (AIP = 5.25 eV), which is consistent with the experimental data [36,46]. The CAl_{12} cluster (40e) exhibits superior stability due to its electronic closed-shell structure with lower EA and higher AIP values. Such phenomenon can be illustrated by their electronic structures according to the Jellium model.

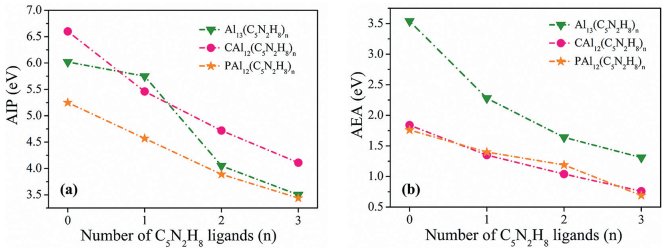

Fig. 3. Calculated AEAs and AIPs of the ligated $XAl_{12}(C_5N_2H_8)_n$ complexes (X = Al, C and P; n = 0-3). All values are given in eV.

The AEAs and AIPs of $XAl_{12}(C_5N_2H_8)_n$ were computed to evaluate the electronic regulation ability of $C_5N_2H_8$. As a result, a successive decline in their AIPs and AEAs with the continuous addition of $C_5N_2H_8$ was observed (Fig. 3). Particularly, the Al_{13} superhalogen cluster changed to a superalkali once the 2nd $C_5N_2H_8$ was attached to the naked cluster. Similar trends were also found in another two clusters, CAl_{12} and PAl_{12}. As shown in Table S3 (Supporting information), the AIP of the closed-shell CAl_{12} cluster reduced from the original 6.60 eV to 4.72 eV in $CAl_{12}(C_5N_2H_8)_2$, and that of the superalkali PAl_{12} cluster continues to decrease to 3.89 eV ($PAl_{12}(C_5N_2H_8)_2$). This finding is interesting because only two $C_5N_2H_8$ ligands can strikingly decrease the AIPs of these aluminum-based superatomic clusters with different shell structures, *i.e.*, 39, 40 and 41 e. Particularly, the Al_{13} and CAl_{12} clusters transform into superalkalis upon the attachment of only two $C_5N_2H_8$ ligands. Additionally, the AIPs of $Al_{13}(C_5N_2H_8)_3$ and $PAl_{12}(C_5N_2H_8)_3$ go further down to 3.50 and 3.44 eV, respectively, which are lower than those of any alkali atoms in the periodic table. These results undoubtedly show that, no matter how their electronic shells are filled (closed or not), $C_5N_2H_8$ exhibits strong power in modulating the electronic properties of these clusters. The conversion between the aluminum-based superatomic clusters and superalkali metals can be attributed to the strong electronic regulation ability of $C_5N_2H_8$, which is not associated with the filling of the electronic shell.

To further understand the origin of the decrease in AIPs of these ligated clusters, we examined their one-electron energy levels (Fig. 4a, Figs. S4a and S5a in Supporting information). It can be seen from Fig. 4a that the continuous increment of the number of the ligand significantly lifts the energy levels of the HOMOs of $Al_{13}(C_5N_2H_8)_n$ (n = 0-3) with the values varying from −5.93 eV to

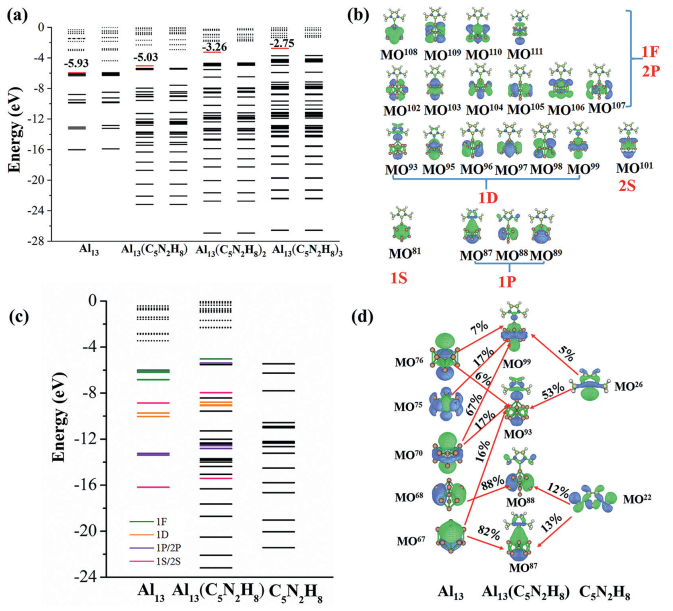

Fig. 4. (a) One-electron energy levels of $Al_{13}(C_5N_2H_8)_n$ (n = 0–3). The red lines indicate the MOs where the ionization occurs; (b) maps of the α occupied MOs of $Al_{13}(C_5N_2H_8)$, where superscripts indicate the orbital numbers; (c) CDA analysis of $Al_{13}(C_5N_2H_8)$ with Al_{13} and $C_5N_2H_8$ as fragments, and their angular characteristics are marked with different colors; (d) isosurface graphs of partial orbital interaction diagram. The numbers marked beside the red lines indicate the contribution from the fragmental MO to the MOs of $Al_{13}(C_5N_2H_8)$. The occupied and unoccupied states in (a) and (c) are illustrated by solid and dashed lines, and the isosurface graphs in (b) and (d) are plotted with an isosurface value of 0.03.

−2.75 eV. It is well-accepted that the ionization process usually occurs in the HOMO of the molecule. Thus, this finding corresponds to the reduction of the theoretical AIPs of $Al_{13}(C_5N_2H_8)_n$ (n = 0-3), which decreases from the original 6.02 eV to 3.50 eV. Similar situations also exist in $CAl_{12}(C_5N_2H_8)_n$ and $PAl_{12}(C_5N_2H_8)_n$ (n = 0-3) (Figs. S4a and S5a). Therefore, it is reasonable to suggest that the prominent decline of the AIPs of $XAl_{12}(C_5N_2H_8)_n$ (X = Al, C and P; n = 0-3), leading to the formation of superalkali clusters, stems from the upward shift of the electronic spectrum.

It is worth noting that, although the successive ligation lifts the energy levels of the metallic core, the order of energy levels in different superatomic MOs almost stays unchanged compared with the bare one. More interestingly, there are no decided change in the H-L gaps during the ligation process (Table S2 in Supporting information), implying that the electronic structures or the shell fillings of the cluster cores may have not been damaged. To verify this conjecture, the MOs of $XAl_{12}(C_5N_2H_8)$ (X = Al, C and P) complexes were carefully checked. Strikingly, all superatomic MOs of these three aluminum-based cluster cores are well preserved and identified. For example, as shown in Fig. 4b, the superatomic MOs of $Al_{13}(C_5N_2H_8)$ are obvious, which is $(1S)^2(1P)^6(1D)^{10}(2S)^2(2P)^6(1F)^{13}$. Similar situations also exist in $CAl_{12}(C_5N_2H_8)$ and $PAl_{12}(C_5N_2H_8)$, as evidenced in Figs. S4b and S5b (Supporting information).

To gain a deeper understanding about the nature of the interaction between the Al_{13} superatomic states and $C_5N_2H_8$, the charge decomposition analysis (CDA), a method based on the concept of fragment orbital to decompose the charge transfer between molecular fragments into the contribution of orbitals, was conducted to evaluate the charge transfer between these two moieties. According to the CDA analysis (Figs. 4c and d), the electron transfer from the ligand to Al_{13} is 0.487e in $Al_{13}(C_5N_2H_8)$, which is consistent with the previous Mulliken analysis. As displayed in Fig. 4c, the frontier 1F and 2P superatomic MOs of the ligated complexes near HOMO have almost no interaction with $C_5N_2H_8$. The energy levels of Al_{13} near the HOMO move upward with the connection of $C_5N_2H_8$. It is prominent that the occupied MO^{93} of $Al_{13}(C_5N_2H_8)$ is responsible for the interactions between Al_{13} and $C_5N_2H_8$, as shown in Fig. 4d. This MO, which is mainly formed by the HOMO (MO^{26}, 53%) of $C_5N_2H_8$ and MO^{67} (16%), MO^{70} (17%), and MO^{76} (6%) of Al_{13}, exhibits the largest electron transfer compared with all other MOs. The MO^{67} (82%) and MO^{68} (88%) of Al_{13} display similar electron characteristic and intermingle with the MO^{22} of $C_5N_2H_8$ leading to the formation of the occupied MO^{87} and MO^{88} of $Al_{13}(C_5N_2H_8)$, respectively. More CDA information and partial orbital interaction diagrams for $CAl_{12}(C_5N_2H_8)$ and $PAl_{12}(C_5N_2H_8)$ are given in Figs. S4c and d, S5c and d (Supporting information), respectively.

Obviously, above findings clearly demonstrate that the electron-donating $C_5N_2H_8$ ligand possesses the power in dramatically dropping the AIPs of typical aluminum-based clusters featuring different shell configurations without disturbing their spueratomic states. Such regulation effect induced by the ligand-field, which is independent of the filling of the electronic shell of the cluster, is completely different from traditional superalkali construction strategies. Importantly, considering the huge application of the ligands in the chemical synthesis of clusters, the present ligand-field strategy cannot only modulate the electronic properties of clusters leading to the formation of novel superalkalis, but also provides promising potential in synthesizing ligated superalklis in the liquid phase. Superior to conventional superatom design strategies that mainly alter the electronic shell filling of the clusters, the current ligand-field strategy has potential to broaden the practical applications of the superatoms. In addition, the $C_5N_2H_8$ ligand was just adopted as a model ligand here, and other ligands featuring similar electron-donating characteristic may also play a part in constructing such superalkali.

In conclusion, the ligand-field strategy, unlike traditional electron counting rules, has been investigated systematically by employing the DFT calculations on the aluminum-based clusters with different shell configurations. During the $C_5N_2H_8$ ligation process, the icosahedral geometries of the metallic moieties, XAl_{12} (X = Al, C and P), remain almost unchanged, indicating that the ligand did not remarkably influence the clusters' structural stability. Relative energetic stability and electronic characteristics of these clusters were also examined. It was observed that the $C_5N_2H_8$ ligand can significantly reduce the AIPs of these aluminum-based clusters without altering their superatomic states. This phenomenon is intriguing because it demonstrates that the regulation effect of such ligand on the clusters' electronic property is irrespective of the filling of the shell configuration of the cluster, which is apparently different from traditional superatom design strategies. The result of the AIP drop may be ascribed to the charge transfer complexes formed by $C_5N_2H_8$, which increases the energy of the HOMO level through the electrostatic Coulomb potential. Moreover, the ligand, rather than just protecting the metallic core from aggregating, can regulate the electronic property of clusters to construct multiple superalkali species. These findings provide potential opportunities for the superatom synthesis in the liquid phase since ligands are widely utilized in the chemical synthesis of atomically precise clusters, which will broaden the practical applications of the cluster-assembly materials. We hope this study will spur further studies about the novel properties and phenomenon of sub-nanoclusters, especially for mimicking the rare/noble elements by using the clusters composed of earth-abundant elements, both in the theory and experiments.

Declaration of competing interest

The authors declare that they have no known competing financial interests or personal relationships that could have appeared to influence the work reported in this paper.

Acknowledgments

This work is supported by the Innovation Project of Jinan Science and Technology Bureau (No. 2021GXRC032), the Taishan Scholars Project of Shandong Province (No. ts201712011), the National Natural Science Foundation of China (NSFC, Nos. 92161101, 21603119), the Natural Science Foundation of Shandong Province (No. ZR2020ZD35), the Shandong University Multidisciplinary Research and Innovation Team of Young Scholars (No. 2020QNQT015), the Young Scholars Program of Shandong University (YSPSDU, No. 2018WLJH48), and the Fundamental Research Funds of Shandong University (No. 2017TB003). The scientific calculations in this paper have been done on the HPC Cloud Platform of Shandong University.

Supplementary materials

Supplementary material associated with this article can be found, in the online version, at doi:10.1016/j.cclet.2022.02.039.

References

[1] J.J. Zhao, Q. Du, S. Zhou, V. Kumar, Chem. Rev. 120 (2020) 9021–9163.
[2] M.T. Huynh, A.N. Alexandrova, J. Phys. Chem. Lett. 2 (2011) 2046–2051.
[3] D.E. Bergeron, P.J. Roach, A.W. Castleman Jr., N. Hones, S.N. Khanna, Science 307 (2005) 231–235.
[4] S.N. Khanna, P. Jena, Phys. Rev. Lett. 69 (1992) 1664–1667.
[5] P. Jena, Q. Sun, Chem. Rev. 118 (2018) 5755–5870.
[6] A.W. Castleman Jr., J. Phys. Chem. Lett. 2 (2011) 1062–1069.
[7] Q. Du, B. Yin, S. Zhou, Z. Luo, J.J. Zhao, Chin. Chem. Lett. 33 (2022) 995–1000.
[8] Z. Luo, A.W. Castleman Jr., Acc. Chem. Res. 47 (2014) 2931–2940.
[9] L. Li, L. Shi, X. Yu, et al., Chin. Chem. Lett. 30 (2019) 1147–1152.
[10] J. Li, H.C. Huang, J. Wang, et al., Nanoscale 11 (2019) 19903–19911.
[11] Q. Liu, P. Fan, Y. Hu, F. Wang, L. Cheng, Phys. Chem. Chem. Phys. 23 (2021) 10946–10952.
[12] Y. Zhao, J. Wang, H.C. Huang, et al., J. Phys. Chem. Lett. 11 (2020) 1093–1099.
[13] A.C. Reber, D. Bista, V. Chauhan, S.N. Khanna, J. Phys. Chem. C 123 (2019) 8983–8989.
[14] D.E. Bergeron, A.W. Castleman Jr., T. Morisato, S.N. Khanna, Science 304 (2004) 84–87.
[15] D. Samanta, M.M. Wu, P. Jena, J. Phys. Chem. Lett. 2 (2011) 3027–3031.
[16] S.B. Cheng, C. Berkdemir, A.W. Castleman Jr., Proc. Natl. Acad. Sci. U. S. A. 112 (2015) 4941–4945.
[17] J.U. Reveles, P.A. Clayborne, A.C. Reber, et al., Nat. Chem. 1 (2009) 310–315.
[18] N.M. Tam, N.T. Mai, H.T. Pham, N.T. Cuong, N.T. Tung, J. Phys. Chem. C 122 (2018) 16256–16264.
[19] W.D. Knight, K. Clemenger, W.A. de Heer, et al., Phys. Rev. Lett. 52 (1984) 2141–2143.
[20] G.N. Lewis, J. Am. Chem. Soc. 38 (1916) 762–785.
[21] I. Langmuir, J. Am. Chem. Soc. 41 (1919) 868–934.
[22] K. Wade, Adv. Inorg. Chem. Radiochem. 18 (1976) 1–66.
[23] B. Pathak, D. Samanta, R. Ahuja, P. Jena, ChemPhysChem 12 (2011) 2423–2428.
[24] I. Langmuir, Science 54 (1921) 59–67.
[25] E. Hückel, Z. Physik 70 (1931) 204–286.
[26] N.C. Baird, J. Am. Chem. Soc. 94 (1972) 4941–4948.
[27] K. Hirata, K. Yamashita, S. Muramatsu, et al., Nanoscale 9 (2017) 13409–13412.
[28] M. Liu, X. Ren, X. Liu, et al., Chin. Chem. Lett. 31 (2020) 3117–3120.
[29] G.X. Liu, A. Pinkard, S.M. Ciborowski, et al., Chem. Sci. 10 (2019) 1760–1766.
[30] X. Fu, X. Lin, X. Ren, et al., Chin. Chem. Lett. 32 (2021) 565–568.
[31] J. Yan, B.K. Teo, N. Zheng, Acc. Chem. Res. 51 (2018) 3084–3093.
[32] J. Li, Y. Zhao, Y.F. Bu, et al., Chem. Phys. Lett. 754 (2020) 137709.
[33] J. Wang, Y. Zhao, J. Li, et al., Phys. Chem. Chem. Phys. 21 (2019) 14865–14872.
[34] J. Li, J. Wang, J. Chen, Y. Bu, S.B. Cheng, CCS Chem. 2 (2020) 1913–1920.
[35] Y. Zhao, J. Chen, H. Yang, Q. Wei, S.B. Cheng, Chem. Phys. Lett. 754 (2020) 137703.
[36] V. Chauhan, A.C. Reber, S.N. Khanna, Nat. Commun. 9 (2018) 2357.
[37] N. Hou, D. Wu, Y. Li, Z.R. Li, J. Am. Chem. Soc. 136 (2014) 2921–2927.
[38] T. Watanabe, K. Koyasu, T. Tsukuda, J. Phys. Chem. C 119 (2015) 10904–10909.
[39] C.A. Smith, M.R. Narouz, P.A. Lummis, et al., Chem. Rev. 119 (2019) 4986–5056.
[40] C.M. Crudden, D.P. Allen, Coord. Chem. Rev. 248 (2004) 2247–2273.
[41] H. Jacobsen, A. Correa, A. Poater, C. Costabile, L. Cavallo, Coord. Chem. Rev. 253 (2009) 687–703.
[42] M.J. Frisch, G.W. Trucks, H.B. Schlegel, et al. Gaussian 09, Revision E. 01; Gaussian, Inc.: Wallingford, CT, 2009.
[43] C. Adamo, V. Barone, J. Chem. Phys. 110 (1999) 6158–6170.
[44] F. Weigend, R. Ahlrichs, Phys. Chem. Chem. Phys. 7 (2005) 3297–3305.
[45] X. Li, L.S. Wang, Phys. Rev. B 65 (2002) 153404.
[46] A.E. Reed, L.A. Curtiss, F. Weinhold, Chem. Rev. 88 (1988) 899–926.
[47] J.E. Carpenter, F. Weinhold, J. Mol. Struct. Theochem. 169 (1988) 41–62.
[48] T. Lu, F. Chen, J. Comput. Chem. 33 (2012) 580–592.
[49] W. Humphrey, A. Dalke, K. Schulten, J. Mol. Graph. 14 (1996) 33–38.
[50] A.C. Reber, S.N. Khanna, P.J. Roach, et al., J. Am. Chem. Soc. 129 (2007) 16098–16101.
[51] X. Li, A. Grubisic, S.T. Stokes, et al., Science 315 (2007) 356–358.
[52] S.B. Cheng, C. Berkdemir, A.W. Castleman Jr., Phys. Chem. Chem. Phys. 16 (2014) 533–539.
[53] Y. Wang, J.M. Holden, A.M. Rao, et al., Phys. Rev. B 45 (1992) 14396–14399.